Rock Mech. Rock Engng. (1995) 28 (2), 69–92

Rock Mechanics and Rock Engineering

Towards an Understanding of Joint Roughness

By

J. P. Seidel and **C. M. Haberfield**

Department of Civil Engineering, Monash University, Clayton, Australia

Summary

It is argued that the currently available joint models are incapable of accurate predictions of joint shear behaviour without resorting to substantial levels of empiricism. This is because these models fail to adequately quantify joint roughness, or appreciate the importance of scale. A novel approach, which uses fractal geometry to investigate joint roughness, is described. This approach goes beyond describing the "symptoms" of roughness and seeks to find the "cause". In the application of this approach, the concepts of fractal geometry, fractal dimension and self similarity are described and used as a framework to formulate a statistically based and practical model for the characterisation of rock joint roughness. Important relationships between the fractal dimension and the more useful statistical parameters of standard deviation of both asperity angles and asperity heights are derived. These relationships not only provide a useful, working method for quantifying joint roughness, but are also shown to provide a basis for understanding the Barton empirical JRC-JCS model. In addition, the fractal model is able to provide conceptual models for the effects of normal stress on the shear behaviour of joints and the scale-dependence of joints.

1. Introduction

Joint roughness is of paramount importance to the shear behaviour of rock joints. This is because joint roughness has a fundamental influence on the development of dilation, and as a consequence, the strength of the joint during relative shear displacement. To date, perhaps due to the earlier work of Patton (1966), joint roughness has been considered as a parameter that effectively increases the friction angle of the joint above the base friction angle, ϕ_b, by some "asperity" or "dilation" angle, usually designated by i, i.e.

$$\tau = \sigma \tan (\phi_b + i), \tag{1}$$

where τ is the shear strength of the joint and σ is the average normal stress on the joint. In fundamental terms, i, can be interpreted as the angle of dilation of the joint during shearing. Typically, for rough rock joints, the value of i is not constant, but gradually decreases with increasing shear displacement. The

variation in i is due to the random and irregular surface geometry of natural rock joints, the finite strength of the rock, and the interplay between surface sliding and asperity shearing mechanisms.

The majority of the research carried out to date has concentrated on the quantification of joint roughness by searching for representative values of i, or the variation of i with shear displacement. A wide variety of techniques have been adopted, including, amongst others, empirically based methods (Bandis et al., 1983), tribology (Wu and Ali, 1978), autocorrelation functions and spectral density functions (Wu and Ali, 1978; Krahn and Morgenstern, 1979) and fractal geometry (Lee et al., 1990; Huang et al., 1992). However, it appears that there is no practical, objective, method available that can accurately quantify roughness for use in joint models.

Perhaps this is partly due to the scale-dependence of roughness. A joint subjected to small shear displacement will be primarily influenced by small scale roughness. However, the same joint undergoing large shear movements will be governed by large scale roughness components. Similarly, as shown by Barton and Bandis (1982), small lengths of joint will be affected by small scale roughness and large joint lengths by large scale roughness. In order to predict the full shear behaviour, therefore, a single roughness statistic will be inadequate.

A careful study of the currently available descriptions of roughness indicate that roughness has been treated from a very limited perspective – looking at and describing the "symptoms" of roughness rather than seeking the "cause". What is needed is a philosophy which, as a minimum, can provide a qualitative appreciation of the nature of roughness, and which can provide an insight into the meaning of roughness at different scales. Armed with such an understanding, a quantitative description of roughness, suitable for incorporation into theoretically based models of joint behaviour, should be possible.

In this paper, the beginnings of such an understanding, based on the concepts of fractal geometry, are outlined. The formulation of a theoretical and practical model of roughness, based on fractal geometry, is described. This model is applied to the problem of scale in rock joints and is shown to provide a basis for understanding Barton's empirical JRC-JCS joint model (Bandis et al., 1983; Barton and Choubey, 1977).

2. Existing Descriptions of Roughness

Given the importance of roughness in controlling the shear behaviour of rock joints, it is not surprising that a large number of researchers have attempted to characterise joint roughness, develop systems to quantify roughness, and relate roughness to shear behaviour.

Perhaps the most widely used is the empirical approach proposed by Barton and Choubey (1977). They addressed roughness in terms of a Joint Roughness Coefficient (JRC) that could be determined either by tilt, push or pull tests on rock samples or by visual comparison with a set of roughness profiles. These roughness profiles were obtained from a series of 136 joint specimen tests carried out on

samples of approximately 100 mm length. Samples were grouped in ranges of JRC 0–2, 2–4, etc. up to 18–20, depending on performance measured during shear tests. One typical profile from each group was selected for a set of representative roughness profiles. This set of profiles has subsequently been adopted as a standard by the ISRM (1978). On the basis of their extensive laboratory testing, Barton and Choubey (1977) proposed the following expression for prediction of joint peak shear strength:

$$\tau = \sigma_n \tan\left[\mathrm{JRC}\log_{10}\left(\frac{\mathrm{JCS}}{\sigma_n}\right) + \phi_b\right] \tag{2}$$

where τ = peak shear strength
σ_n = normal stress on the joint
JRC = joint roughness coefficient
JCS = joint wall compressive strength
ϕ_b = base friction angle of the rock.

Equation (2) is the same as the Patton model (Eq. (1)) but with $i = \mathrm{JRC}\log_{10}(\mathrm{JCS}/\sigma_n)$. This implies that JRC is essentially an empirically determined dilation angle. A correction to this dilation angle is made to account for normal stress ($\log 10(\mathrm{JCS}/\sigma_n)$ in Eq. 2).

It should be noted that Eq. (2) has subsequently been modified by Barton and his colleagues in a number of important ways. Barton and Bandis (1982) introduced empirically-derived scale corrections based on limited laboratory testing of joints of varying length to derive the scale dependent values JRC_n and JCS_n. Bandis (1993) included an additional term i_u in the basic formulation to account for large scale joint undulations. Furthermore, Barton and Bandis (1990) noted that dilation angles, d_n, may reduce to as low as $d_n = 0.5\mathrm{JRC}\log_{10}(\mathrm{JCS}/\sigma_n)$ at high normal stress levels due to the effects of asperity damage.

Rengers (1970) and Feker and Rengers (1971) proposed a method to capture the statistical aspects of joint roughness. The method consists of choosing a reference line parallel to the general direction of the joint. The joint is then digitised (typically at 1 mm intervals), and the profile is traversed in discrete steps, recording the maximum positive and negative angles over the profile. The step length is progressively increased, and the tangents for the maximum positive and negative angles for each step size are plotted. The data can also be represented as a hypothetical "free" dilation curve which represents the maximum possible dilation that can occur for any given relative shear movement.

This innovative method is effective in addressing roughness as a parameter which is subject to scale effects. However, as it does not incorporate any aspects of rock strength, its value as a predictive tool is limited to either hard rocks, where little surface degradation occurs at moderate stress levels, or to softer rocks with very low stress levels. Furthermore, the concept of free dilation angles for step-lengths exceeding the longest underlying wavelength in a joint, probably has little physical relevance.

Williams (1980), in his research on rock socketed piles, samples the roughness of wall sockets and quantified the socket profiles as a set of statistics of roughness angles and heights for 2 mm step lengths. Haberfield and Johnston (1994)

adopted a similar procedure in their model of joint behaviour. However, instead of keeping a constant step length, they proposed that a roughness profile obtained from a typical joint cross-section could be idealised as a series of variable length, straight lines. For example, the joint profile, shown as a dashed line in Fig. 1, could be idealised as the series of straight lines or chords depicted by the solid line, also shown in Fig. 1. Haberfield and Johnston noted that such a typical joint profile is but one of an infinite number of cross-sections of the same joint surface and that other joint cross-sections would result in different straight line profiles. They suggested that each idealised profile could then be analysed (independently or collectively) on a statistical basis to obtain four roughness parameters – the mean and standard deviation of the chord absolute inclinations, and the mean and standard deviation of chord end-point absolute heights.

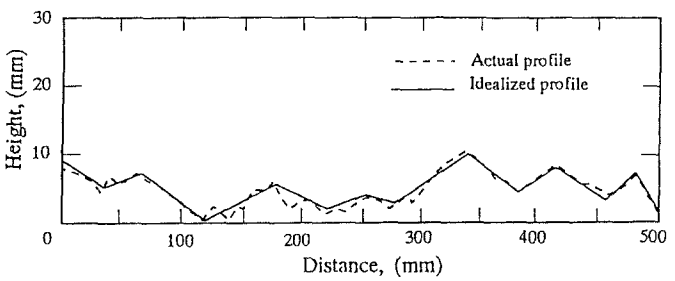

Fig. 1. Natural rock joint and corresponding idealisation (after Haberfield and Johnston, 1994)

They also noted that the way in which a profile is idealized is subjective. Furthermore, the method gives no guidance as to what constitutes an appropriate scale for idealization. A particular idealization may be appropriate if shear movements of 20 mm are to be modelled, but entirely unsatisfactory if movements of only 2 mm or as much as 200 mm are anticipated.

Apart from the large body of work relating surface parameters to friction in the field of tribology and wear theory, e.g. Koura and Omar (1981), many other investigators (Wu and Ali, 1978; Krahn and Morgenstern, 1979; Williams, 1980; Tse and Cruden, 1979; Reeves, 1985) have specifically attempted to correlate surface roughness with the frictional behaviour of rock joints by statistical methods. As noted by Reeves (1985), the statistical parameters used can be divided into two categories:

- those describing the magnitude of roughness; namely the centre-line roughness and root mean square roughness;
- those describing the texture of the rough surfaces, namely the root mean squares of the first and second derivatives of the surface profile, autocorrelation function, spectral density function, mean square value and structure function.

The autocorrelation function indicates the general dependence of the values at one position on the values at another position, and is therefore useful in detecting persistent cyclic functions embedded in a complex profile. The spectral density

function, which is the Fourier transform of the autocorrelation function, is similarly an indicator of periodicity.

Krahn and Morgenstern (1979) attempted to relate a number of these roughness parameters to either the "peak" or "ultimate" (i.e. large strain) friction angles of lapped, dry-sanded or diamond saw cut surfaces of limestone. At best, a correlation coefficient of 0.881 was achieved between the first derivative of the surface profile and the ultimate friction angle. All other correlations were statistically insignificant.

Tse and Cruden (1979) were attracted by the development of correlations between various statistical parameters and Barton's roughness charts, which they digitised. Eleven empirical correlations were investigated, and these varied from very poor to excellent. Despite the high coefficient of correlations for some of these statistics, the value of empirical correlations with the JRC factor (which is itself empirical and scale dependent) must be questioned. Others (e.g. Wu and Ali, 1978; Reeves, 1985; Yu and Vayassade, 1991) have also been motivated to examine these roughness profiles.

Recently, a number of researchers (Lee et al., 1990; Turk et al., 1987; Carr and Warriner, 1987) have applied the concept of fractal dimension to rock joints. Lee et al. (1990) and Turk et al. (1987) applied the concept of fractal dimension to natural and artificially created joints, and to an analysis of the ISRM standard roughness profiles (ISRM, 1978). Lee et al. determined an empirical relationship between JRC and the fractal dimension, D, as follows:

$$\text{JRC} = -0.87804 + 37.7844\left(\frac{D-1}{0.015}\right) - 16.9304\left(\frac{D-1}{0.015}\right)^2. \tag{3}$$

Turk et al. (1987) took an alternative approach, and developed a semi-empirical relationship between the average asperity angle, i, and the direct profile length, L_d:

$$\cos i = (XL_d)^{1-D}, \tag{4}$$

where X is a constant, to be established empirically. In their analyses, Turk et al. found that the fractal dimension was not constant over the range of step lengths investigated (2, 6, 20 and 60 mm), so they adopted a standard step length of 6 mm. On this basis, for the ISRM standard profiles, they determined constants varying unsystematically from $X = 20.9$ to $X = 99.1$ for each group of JRC values.

The approaches described above, which are based on the representation of roughness as a single statistic, or a limited set of statistics, cannot hope to capture the complexities of joint behaviour, and the interplay of both geometrical and strength properties of rock joints. Their use must be coupled with empirical factors which are at best approximate.

If a fundamental approach to the shear behaviour of rock joints is sought, it must be matched with a fundamental understanding and quantification of roughness. As will be explained, fractal geometry provides a framework to develop such an understanding.

3. Fractal Geometry

As fractal geometry is central to the development of the roughness model, a brief introduction to the concepts of fractal geometry has been included. Further details can be obtained from any of a number of references on the topic; e.g. Kaye (1989), Mandelbrot (1977, 1983).

Fractal geometry is the geometry of "chaos theory", and has been described as the geometry of Nature. Nature rarely presents itself in the shapes of Euclidean geometrical forms – straight lines, triangles, squares, etc. – but rather in forms which can be considered as chaotic. Clouds, trees, mountain ranges, coastlines and rock joints have not been engineered, but are a result of the conjunction of unknown and random forces. All are poorly represented in terms of classical geometrical concepts, but lend themselves to probabilistic representation using fractal geometry.

Fractional Dimensions

Euclidean geometry deals with objects which can be described in integer dimensions. A straight line is one dimensional, a square or triangle are two dimensional, and a cube or rhomboid are three dimensional. Thus, if a straight line of unit length is divided into chords of length, r, as shown in Fig. 2a, then the number of segments, N, and the chord length can be related as follows:

$$N = \frac{1}{r^1}. \tag{5}$$

Similarly, as shown in Fig. 2b, if a unit square is divided into smaller squares of side, r, the total number of squares is

$$N = \frac{1}{r^2}. \tag{6}$$

And, for the unit cube shown in Fig. 2c

$$N = \frac{1}{r^3}. \tag{7}$$

If the parameter, D, is defined as the dimension, the following general relationship can be determined:

$$N = \frac{1}{r^D} \quad \text{or} \quad Nr^D = 1. \tag{8}$$

Nature, however, is not so obligingly regular. Mandelbrot (1983) describes early work by Richardson (1961), in which he discovered that the length of the coastlines and borders of a range of countries was not constant, but increased, apparently without limit, the smaller the measuring step used.

It can be appreciated that maps at increasingly smaller scales will reveal ever smaller bays and promontories that must be traversed and that were not apparent at the larger scales. Whatever the specific detail at a particular scale, it is apparent that the general form at all scales is smaller, and appears to reflect

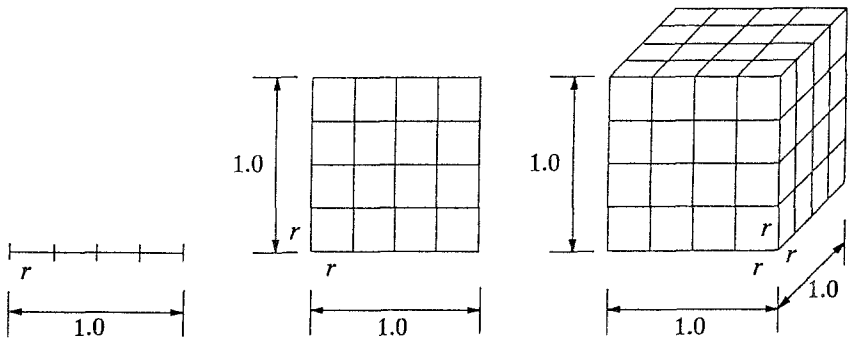

a) Unit Length $N = 1/r$

b) Unit Square $N = 1/r^2$

c) Unit Cube $N = 1/r^3$

Fig. 2. The concept of dimension in Euclidean geometry

specific mechanisms that created both small and large details. This example leads to two important concepts – that of the fractional (or fractal) dimension, and that of self similarity.

The problem of the increasing coastline length implies that the number of steps required to traverse the entire length is not inversely proportional to step length, as would be expected for a one-dimensional line. Therefore, even though the *topological* dimension of the line is always 1, the dimension D in Eq. (8) is fractional, and greater than 1. Rearranging this equation, we obtain an expression for the fractal dimension, D as follows:

$$D = -\frac{\log(N)}{\log(r)}. \tag{9}$$

Graphically, the fractal dimension can be obtained from the slope of a log–log plot of step number, N, against step length, r. Alternatively, a log–log plot of trace length, L, against r will have a slope of 1-D.

The other important concept that can be appreciated from the coastline example is that the irregularities of the coastline as a whole seen at the largest scale are mirrored in the irregularities of the bays or promontories visible at smaller scale, and even, in the limit, theoretically in the tide line that contacts with the sand grains on the beach.

The term "statistical self-similarity" was coined by Mandelbrot (1977) to denote similarity at a range of scales in a *statistical* rather *geometrical* sense. The stronger form of "self-similarity", which denotes exact geometrical similarity at a range of scales only exists for mathematical constructions.

A classical example of such mathematical constructions is Koch's triadic island, shown in Fig. 3. The starting point in the construction is an equilateral triangle. Each side is split into three parts ($r = 1/3$). The centre part is removed, and replaced by two new sections, each equal in length to the part removed, and now forming a "tent" at the middle of each side ($N = 4$). This geometric

construction increases the length of each side of the triangle by a factor of 4/3. The result of this transformation on all sides is the "Star of David" denoted as the second stage. The third stage is developed using the same technique of increasing the length of each face by the factor 4/3. The process continues to the N^{th} stage, at which a form very much resembling a snowflake is generated.

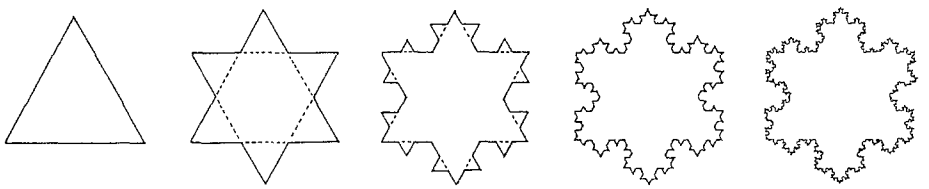

Fig. 3. Construction of the N^{th} order Koch's triadic island (after Mandelbrot, 1983)

It should be noted that the Koch triadic island satisfies the criterion of self-similarity, since it has exact geometrical similarity at all scales, i.e. if a very small portion of the perimeter of the triadic island is magnified, then it would look exactly the same as the original large part of the boundary. Secondly, the fractal dimension of Koch's triadic island, according to the definition in Eq. (9), is $D = -\log(4)/\log(1/3) = 1.2618$. It can further be appreciated that in the limit, the length of the perimeter is infinite, although the area contained by the triadic island is finite.

Empirical Determination of Rock Joint Fractal Dimension

The similarity of the roughness of rock joints to the roughness of coastlines is evident on an intuitive basis, and as stated earlier, the application of the concept of the fractal dimension to rock joints has been pursued by many researchers, e.g. Lee et al. (1990), Turk et al. (1987) and Carr and Warriner (1987).

Lee et al. (1990) and Turk et al. (1987) determined the fractal dimension of the standard ISRM joint profiles using the so-called "compass walking" method. A compass or set of dividers of constant opening, r, is walked over the profile, and the number of complete steps and fractional remainder steps are recorded. Turk et al. (1987) determined fractal dimension manually, while Lee et al. (1990) appear to have enlarged the profiles to twice their original size, and then digitised these profiles for analysis by a computer program which digitally performs the same compass walking process.

It is interesting to compare the fractal dimensions determined by the two research groups in Table 1. Also shown in this table are values determined by the authors in a manner similar to the digitising method of Lee et al. (1990). The table shows that the fractal dimensions of even the roughest profiles are marginally greater than 1. However, small values are to be expected, since the difference between the topological dimension of a line (1) and its fractal dimension ($1 \leq D \leq 2$) is a measure of its space-filling ability. Thus a straight line has both a topological and fractal dimension of 1, whereas Brownian motion, which has

complete space filling ability, has a topological dimension of 1 and a fractal dimension of 2.

Table 1. Estimated fractal dimensions for ISRM standard roughness profiles

JRC	Lee et al.	Turk et al.	Current study
0–2	1.000446	1	1.00009
2–4	1.001687	1.0019	1.00054
4–6	1.002805	1.0027	1.00072
6–8	1.003974	1.0049	1.0014
8–10	1.004413	1.0054	1.0018
10–12	1.005641	1.0045	1.004
12–14	1.007109	1.0077	1.0053
14–16	1.008055	1.007	1.0081
16–18	1.009584	1.0104	1.0096
18–20	1.013435	1.017	1.012

The fractal dimensions reported in Table 1, although showing similar trends, do vary considerably for individual profiles, given the accuracy which is suggested by the number of significant figures reported. It is considered that these differences are due to inaccuracies both with the physical difficulties of compass stepping on the one hand, or on the other hand, manually guiding a digitiser over the profiles with finite width. It is thought that some of the variation may have arisen from differences in the arbitrary choice of step length. The relevance of all determinations of fractal dimensions is also compromised by the succession of reproductions made since the tracing of the original profiles by Barton and Choubey (1977).

It should also be noted that considering the small differences between trace length and direct length that these low fractal dimensions imply, small errors in length measurement will result in relatively large errors in the fractal dimension computed.

The Fractal Dimension of "Self-Affine" Surfaces

The general application of (particularly) the compass-walking method has generated a large amount of controversy in the technical literature (Huang et al., 1992; Mandelbrot, 1985). Huang et al. (1992) note that fractal surfaces may be "self-affine" (a term coined by Mandelbrot, 1977) rather than statistically self-similar. Mandelbrot (1985) suggested that rock surfaces are theoretically self-affine. The difference between the two terminologies is that a self-similar surface is statistically equivalent when scaled equally in both axial and transverse directions, whereas a self-affine surface must be scaled differently in perpendicular directions to maintain statistical similarity. For a self-similar fractal such as the Koch triadic island, compass walking will always define the similarity dimension. However, for a self-affine surface, the fractal dimension can only be determined for step lengths less than a critical length, known as the cross-over length. Above

this length, step-dividing will always produce a bogus fractal dimension approaching unity[1].

As noted previously, rock joints are essentially self-affine surfaces. They are generally linear structures, comprising (many) segments which may in themselves be statistically self-similar without the joint length *as a whole* being self-similar. The determination of the joint's fractal dimension will only be valid at step lengths less than the cross-over length (which must be established).

4. The Fractal Dimension and Roughness Statistics

As an index in itself, the fractal dimension is of little use to the practicing engineer interested in describing and quantifying the aspects of roughness which govern the behaviour of rock joints. It is therefore necessary to develop methods which relate fractal dimension to common roughness statistics such as step or chord angle and height.

With the Koch triadic island introduced earlier, the "initiator" is a constant geometric transformation which is applied to every line in each successive generation. Mandelbrot (1983) develops the concept of the Peano curve. The simple Peano curve initiator is a pair of segments each emanating from the original chord endpoints at 45° to the chord, and meeting above the chord midpoint at right angles as shown in Fig. 4a. The fractal dimension of this initiator is $D = -\log(2)/\log(1/\sqrt{2}) = 2.0$ A degree of randomness can be introduced into this initiator by allowing the initiator to "flip-flop" randomly on either side of the chord, as shown in Fig. 4b. The fractal dimension remains the same. This is further developed by Mandelbrot by maintaining a right angle connection between the two initiator segments, but allowing the angle subtended by one of the segments with the initial chord to vary randomly between 0° and 360°, as indicated in Fig. 4c. This final development results in a fractal which has statistical rather than geometric self-similarity.

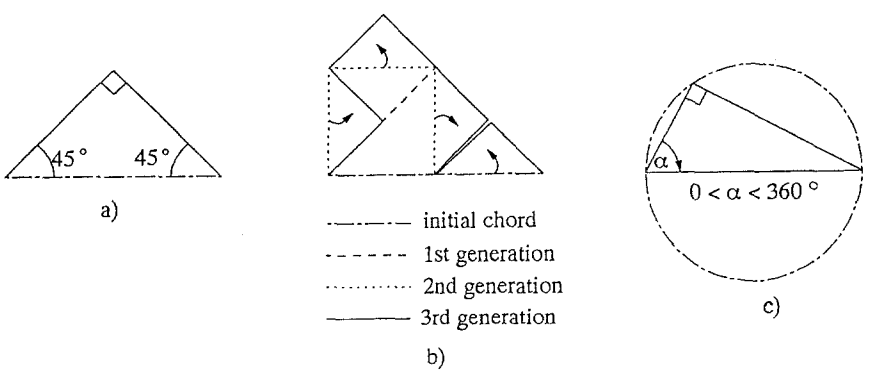

Fig. 4. The Peano curve and successive stages of randomisation (after Mandelbrot, 1983)

[1] c.f. comments on free-dilation angle of Feker and Rengers at large step lengths.

The Fractal Dimension and Standard Deviations of Angle and Height

Similar concepts to Mandelbrot's randomisation of the Peano curve have been applied by the authors to develop a relationship between fractal dimension and the statistics of angle and height applicable to surfaces such as rock joints. Other researchers have attempted to determine relationships between JRC and fractal dimension that are partly or wholly empirical. However, in an attempt to understand the true nature of roughness, and hence extract the relevant statistics to characterise rough surfaces, a theoretical basis for understanding the relationship between fractal dimension and asperity angles was sought.

Assume that a joint profile of unit direct length can be characterised by N segments or chords of constant length, r, as shown in Fig. 5. For convenience, let the joint profile be oriented such that the direct line joining its two end points is horizontal. Starting at the left hand end of the profile, each chord can therefore be defined in turn, by its inclination, θ, measured relative to the horizontal, and the chord length, r. Based on roughness measurements of rock joints carried out by Reeves (1985) and others, it is reasonable to assume that the distribution of chord angles, θ, is gaussian, with menu, μ_θ, and standard deviation, s_θ. As the line joining the start and end points of the joint profile is horizontal, then $\mu_\theta = 0$, which implies that the chord angles are normally distributed about the horizontal. Positive angles are assumed to be inclined upwards from left to right.

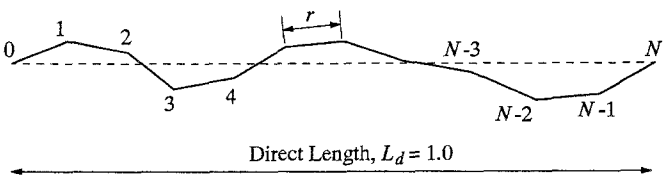

Fig. 5. Characterisation of a profile of unit length with chord length r

Referring to Fig. 6, the horizontal component of chord length is $l = r\cos\theta$. Since the joint profile is of unit length and there are N chords, the mean of the horizontal component of chord lengths, $\mu(l) = 1/N$. However, since r is constant, then $\mu(l) = r\mu(\cos\theta) = 1/N$. For a normal distribution of chord angle, the distribution of the angle cosines is not normal, since $\cos\theta = \cos(-\theta)$. However, it has been shown (Seidel, 1993) that for a large population, the mean of the cosine of chord angle approximates to the cosine of the standard deviation of chord angle, i.e.

$$\mu(\cos\theta) \approx \cos(s_\theta). \tag{10}$$

Substituting for $\mu(\cos\theta)$, leads to a relationship between step length, r, number of segments, N, and the standard deviation of segment angle, s_θ:

$$r \approx \frac{1}{N\cos(s_\theta)}, \tag{11}$$

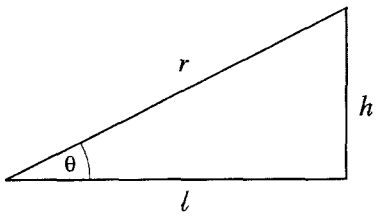

Fig. 6. Single chord geometry

however, by definition

$$D = -\frac{\log(N)}{\log(r)}.$$

Hence, substituting for r and rearranging, leads to

$$s_\theta \approx \cos^{-1}(N^{(1-D)/D}), \tag{12}$$

which implies that the standard deviation of chord angle is a function only of the number of chords and the fractal dimension. For $s_\theta \leq 20°$ (equivalent to JRC ≤ 20 at a 1 mm scale), the error associated with the inequalities in Eqs. (10) and (12) are less than 0.1% (Seidel, 1993). It should be noted that a value of $s_\theta = 20°$ does not represent an absolute limit, and at very small scales, values of s_θ in excess of 20° may be common. However, this level of roughness implies that the joint will contain very steep asperity angles in excess of 60° (3 standard deviations), which will fail by shearing rather than sliding.

The variation of s_θ with the number of chords, for a range of fractal dimensions, is shown in Fig. 7. It can be seen that in the limiting case of $N = 1$ (one chord only), $\theta = 0°$, regardless of the fractal dimension, which is correct, as any two points connected by a single line must be straight. Further, for a fractal dimension of 1, $\theta = 0°$ by definition, regardless of the number of chords into which the profile is subdivided. This is to be expected, since a fractal dimension of 1 (equal to the topological dimension) implies a straight line.

For the more general case of fractal dimension, $D > 1$, it can be seen (from Fig. 7) that the standard deviation of chord angle increases both with the fractal dimension, which can be interpreted as the tendency for divergence from a straight line, and N, which can be interpreted as the number of opportunities for divergence.

It is important to note that this model implies that rough surfaces have an innate tendency for the asperities to diverge from straightness, which can be quantified by the fractal dimension, and which increases with increasing fractal dimension.

The corollary to the establishment of a relationship between fractal dimension and standard deviation of chord angle is that a similar relationship can be established for the standard deviation of chord height, s_h. From Fig. 6, $h = r\sin\theta$. Since r is constant, then $s_h = rs(\sin\theta)$, where $s(\sin\theta)$ is the standard deviation of the sines of the chord angles. However, it can also be shown (Seidel, 1993) that for a large population, $s(\sin\theta) \approx \sin(s_\theta)$ which leads to $s_h \approx r\sin s_\theta$ and Fig. 8.

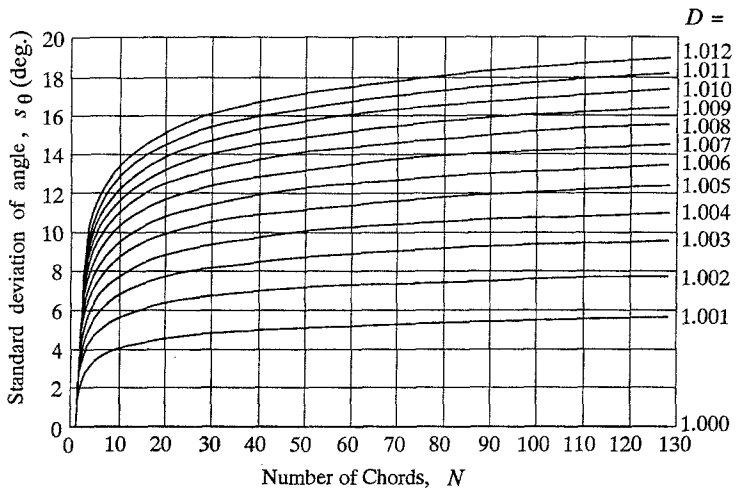

Fig. 7. Graphical representation of Eq. (12) – variation of standard deviation of angle

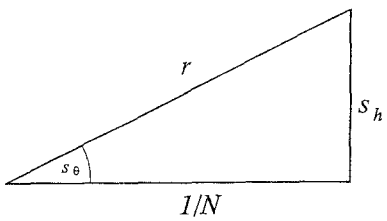

Fig. 8. Definition of standard deviation of chord length

From Fig. 8 it is clear that

$$r \approx \sqrt{s_h^2 + \frac{1}{N^2}} \tag{13}$$

and, from the definition of fractal dimension,

$$D \approx -\frac{\log(N)}{\log\left(s_h^2 + \frac{1}{N^2}\right)^{1/2}}. \tag{14}$$

By rearranging terms, an approximate relationship between fractal dimension and the standard deviation of segment height can be established:

$$s_h \approx \sqrt{N^{-2/D} - N^{-2}}. \tag{15}$$

The error in the equality of Eq. (15) is less than 1% for $s_\theta < 10°$ and less than 4% for $s_\theta < 20°$ (Seidel, 1993).

As for the standard deviation of chord angle, the implication for the standard deviation of chord height in the limiting cases of fractal dimension, $D = 1$ or when the number of chords, $N = 1$, is in both cases a chord height of 0, as expected for a straight line. For a line of direct length, L_d, rather than unity, the standard

deviation of height is given as:

$$s_h \approx L_d \sqrt{N^{-2/D} - N^{-2}}. \tag{16}$$

It should be stressed that these relationships are valid only to *that portion of a joint or interface which can be considered as self-similar*. A generalised joint surface must be analysed in order to determine what is the underlying fundamental "wavelength" or "cross-over length" above which the profile is no longer fractal, but in a statistical sense, repeats itself. Furthermore, the height and angle statistics are seen to be intimately related, and are not independent variables, as has been assumed by others.

5. Generation of Roughness Profiles

As discussed previously, a number of researchers (Lee et al., 1990; Turk et al., 1987) have attempted to compute the fractal dimension of the ISRM standard roughness profiles and then correlate these with the JRC.

A reverse approach has been taken here in attempting to understand the significance of the ISRM profiles. Using the technique of mid-point displacement (Mandelbrot, 1983) and using the techniques for generating random numbers with gaussian distribution described by Stevens (1990), it is possible to generate roughness profiles that depend only on the number of subdivisions, N, and the fractal dimension, D. The technique is depicted graphically in Fig. 9.

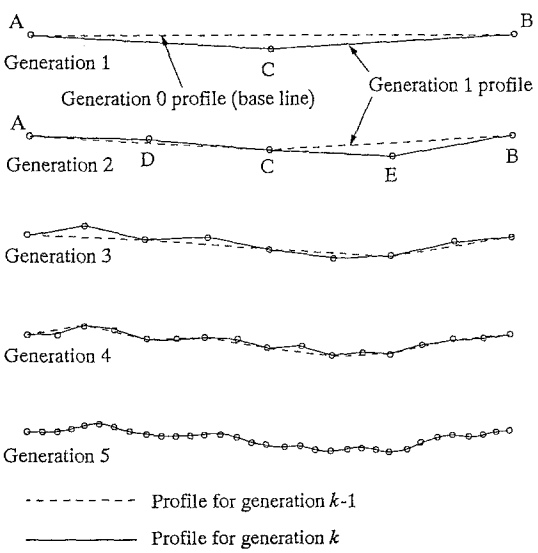

Fig. 9. Generation of random roughness profiles using mid-point displacement technique

For a line AB of given length, the number of chords, N, into which the line is to

be divided is chosen, with the restriction that N is a positive integer power of 2, i.e. $N = 2^k$; $k \geq 1$. Given N and the standard deviation of angle, s_θ, the fractal dimension, D, and the standard deviation of chord heights, s_h, can be determined from Eqs. (12) and (16) respectively. The profile generation is initiated by displacing the midpoint of AB (i.e. point C) vertically a height, h, in accordance with the chosen gaussian distribution (see Fig. 9). Note that h can be positive or negative, with a negative value indicating a downward displacement. The actual height and sign of the displacement is chosen randomly from a gaussian population. This procedure is analogous to the first stage initiation of the Koch triadic island or the Peano curve, both of which have been discussed earlier.

As the number of segments being created in the first generation is 2, the standard deviation of height is given by:

$$s_{h,1} \approx L_d \sqrt{2^{-2/D} - 2^{-2}}. \tag{17}$$

In the next step, the intervals AC and CB are also bisected, and their respective midpoints (D and E) are similarly allowed to displace on either side of their respective chords according to a random choice from a gaussian population. However, because the chord lengths in this case have been halved, the standard deviation of the applied displacement in this second generation will only be half of the displacement applied in the first generation, i.e.

$$s_{h,2} \approx \frac{L_d}{2} \sqrt{2^{-2/D} - 2^{-2}}. \tag{18}$$

A general expression for the standard deviation of mid-point displacements for the kth bisection can be expressed as follows:

$$s_{h,k} \approx L_d \sqrt{2^{-2(1+kD-D)/D} - 2^{-2k}}. \tag{19}$$

Equations (19) and (16) differ in that the term s_h in Eq. (16) incorporates the height variability due to all roughness of scale greater than or equal to the k^{th} bisection, whereas $s_{h,k}$ in Eq. (19) is specific to the component of roughness attributable only to the k^{th} bisection.

This process of successive bisection of segments, and displacement of the midpoints according to gaussian distributions, continues until the original chord has been divided into the pre-determined number of chords, N.

It is important to note that the process of successive bisection of the original chord maintains the self-similarity of the profile in a statistical sense. With each new bisection, further opportunities are given for the segments to diverge from the original chord; new gaussian distributions are superimposed upon the previous gaussian distribution. Figure 10 shows the effect of this superposition for the 2$^{\text{nd}}$ and 3$^{\text{rd}}$ bisections. In each case, the net distribution resulting is still a gaussian distribution, confirming the element of self-similarity, however, the standard deviation increases with each successive bisection. This can be shown from the addition theorem of variances, i.e.

$$s^2 = s_1^2 + s_2^2. \tag{20}$$

As the two variances (of segment angle) being superimposed are equal, it follows that

$$s^2_{\theta,2} = 2s^2_{\theta,1}, \tag{21}$$

where $s^2_{\theta,2}$ is the variance of angle for the 2nd bisection. More generally for the k^{th} bisection, the standard deviation of angle can be determined as follows:

$$s_{\theta,k} = \sqrt{k}\, s_{\theta,1} \approx \sqrt{k} \cos^{-1}(2^{(1-D)/D}). \tag{22}$$

The close correspondence of Eq. (22) and Eq. (12) is noted. Their approximate identity can be verified by substitution of $N = 2^k$ in Eq. (12).

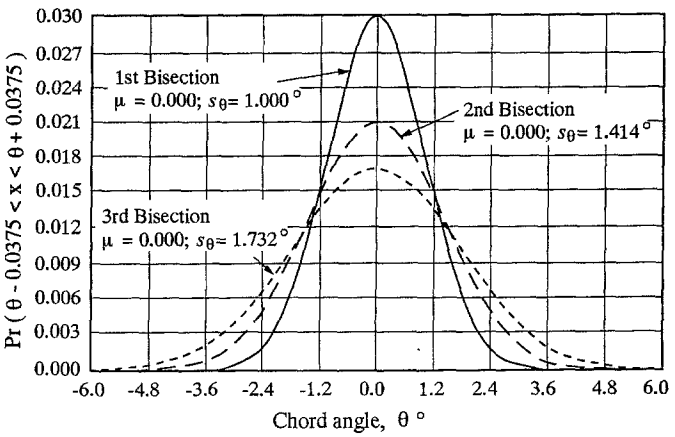

Fig. 10. Chord angle distribution for successive chord bisections

Although, as shown below, the process of mid-point displacement can produce realistic roughness profiles, it must be pointed out that the profiles so generated, although fractal, are influenced heavily by the initial displacement, and progressively less by subsequent displacements. In practical terms, however, a joint or interface profile would combine many such individual profiles, and the effects would simply be incorporated into the random roughness of the surface.

It should also be noted that for a gaussian distribution, the mean value of chord angle absolutes $|\bar{\theta}|$, is related to the standard deviation, s_θ, as follows:

$$|\bar{\theta}| = \sqrt{\frac{2}{\pi}}\, s_\theta. \tag{23}$$

Fractal Profiles and the ISRM Standard Roughness Chart

Examples of typical profiles obtained by applying the mid-point displacement process described above are shown in Figs. 11 to 14. The profiles shown have been generated for standard deviations of chord angle of 3°, 9°, 13° and 17° respectively. All profiles have been generated using 7 random stages of the bisection process, leading to 2^7 or 128 chords in each profile.

Each figure contains 6 profiles. The first five are generated profiles using the same standard deviation of chord angle, but having different "seed" values. The "seed" is a random number, required by, and generated from the random number generator that produces the gaussian distribution of chord heights. Shown at the right hand end of each profile is the actual standard deviation of chord angle for that profile. Note that since only a finite number of chords have been included, the standard deviation of angle obtained will not necessarily be the same as the angle initially adopted, but will be close to it. For example, the profiles shown in Fig. 11, were generated using a standard deviation of chord angle of 3°, whereas the actual standard deviations of the generated profiles range from 2.875 to 3.179°.

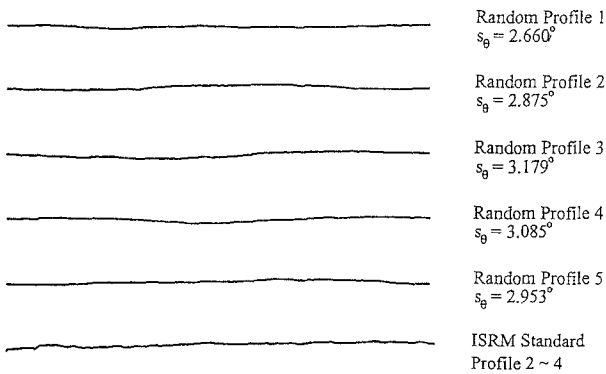

Fig. 11. Random roughness generation for $s_\theta = 3°$ compared with ISRM standard roughness profile JRC 2–4

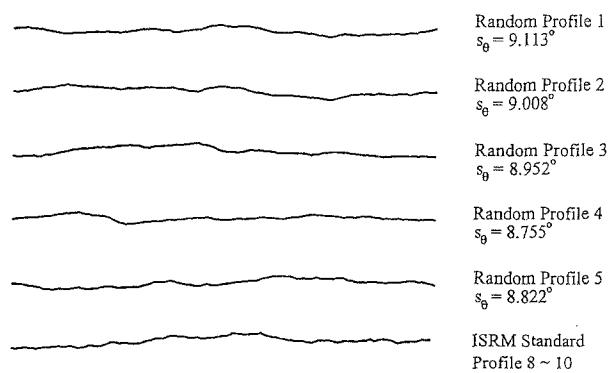

Fig. 12. Random roughness generation for $s_\theta = 9°$ compared with ISRM standard roughness profile JRC 8–10

It should be stated that for the roughest profiles (i.e. $s_\theta = 17°$), profiles were selected on the basis of a small initial displacement for the first generation (see above). It would have been equally possible to characterise these profiles as

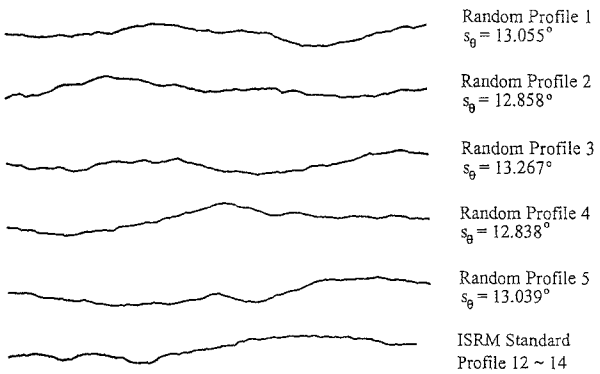

Fig. 13. Random roughness generation for $s_\theta = 13°$ compared with ISRM standard roughness profile JRC 12–14

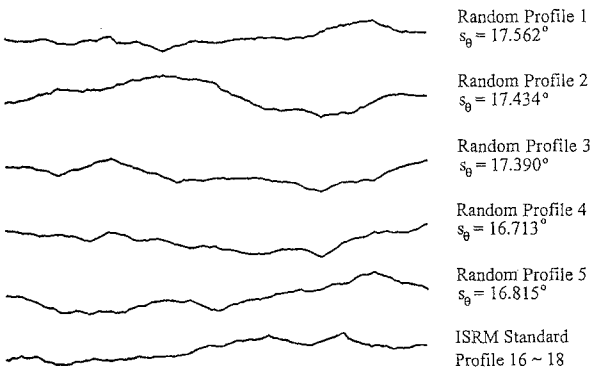

Fig. 14. Random roughness generation for $s_\theta = 17°$ compared with ISRM standard roughness profile JRC 16–18

comprising a number of shorter base lengths, say 4 chords each of 1/4 the original length, and then to have applied 5 random stages of bisection to each of these chords, again resulting in a total of 2^7 chords.

Included with these random profiles, are the ISRM standard roughness profiles for JRC values of 2–4, 8–10, 12–14 and 16–18 respectively. The similarity between the random profiles, based on the fractal dimension, and the ISRM profiles is striking, and suggests a strong correlation between the JRC number and the standard deviation of angle. In fact, the correlation between the standard deviation of angle and JRC has been recognised by others (Williams, 1980; Lam, 1983; Kodikara, 1989). Williams (1980) proposed the following empirical relationship from his analysis of the standard roughness profiles: $\text{JRC} = 0.83 s_\theta$. It is apparent from an examination of successive ISRM profiles (see Figs. 11 to 14) that they show increasing angularity and increasing tendency to diverge from the chord connecting the end points. These are both processes that are mirrored by the generation of random profiles by the mid-point displacement technique.

Roughness Measurement and the Effects of Scale

As illustrated in Fig. 1, it is possible to characterise the major roughness elements of a joint profile by a series of chords of varying length. It is postulated that the average chord length so obtained corresponds to the "cross-over" length. As argued earlier, it is not valid to characterise the profile with chord lengths greater than the cross-over length. However, for chord lengths less than the cross-over length, the profile may be fractal. It follows then, that if the cross-over length can be established, and the angular statistic s_θ is computed for this length, the variation of the standard deviation of angle for smaller lengths can be simply estimated from Eq. (12) without the need for direct determination by accurate digitisation of the rough surface. Conversely, if detailed roughness measurements are available at a range of scales, an appropriate cross-over length can be projected.

The results of predicting a continuum of roughness statistics from only coarse roughness approximations are shown in Fig. 15 for two of the ISRM profiles. The major roughness elements in profiles with JRC 10–12 and 18–20 were (subjectively) identified. This resulted in 4 chords of 25.0 mm average length for the *JRC* 10–12 and 8 chords of 12.8 mm average length for the *JRC* 18–20 profile. Equation (12) was then used to estimate the standard deviation of chord angle for different chord lengths less than the corresponding cross-over length. The results are summarised in Fig. 15, which compares the predicted variation of standard deviation of asperity angles with chord length with values determined from digitisation of the profiles using step lengths as low as 0.2 mm (the profiles were first enlarged considerably). Both comparisons show good agreement, demonstrating that the scale dependence of roughness statistics can be theoretically predicted. The subjectiveness of this procedure as currently proposed is readily acknowledged.

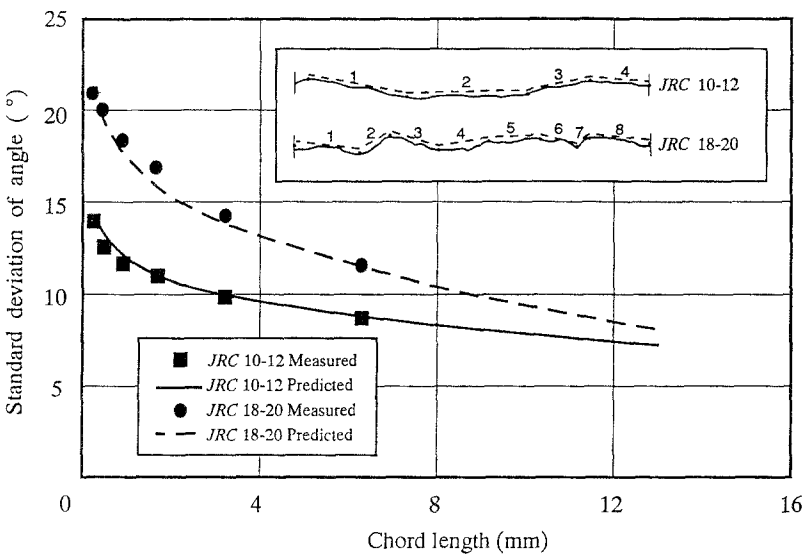

Fig. 15. Comparison of predicted and measured standard deviation of angle for JRC 10–12 and 18–20

6. Understanding Barton's JRC-JCS Model

Standard Deviation of Chord Angle and JRC

It should be noted that the particular standard deviation calculated for the computer-generated profiles discussed above depends on the number of intervals used to generate these roughness profiles. This is because the standard deviation of angle increases with increasing number of subdivisions of the original chord (see Fig. 15). The reason that an apparent equality has been achieved between s_θ and JRC in Figs. 11 to 14 is considered to be because the average segment length of 0.78 mm (128 segments in 100 mm) is close to the peak shear displacements of Barton and Choubey's (1977) test samples. They reported peak shear displacements varying between 0.59 and 1.21 mm, with a mean of 0.95 mm for the 136 samples used in the original study that led to the ISRM standard roughness profiles. The scale of the roughness elements involved in Barton and Choubey's tests are therefore similar to the scale of the generated profiles. It is concluded that the standard deviation of angle *at a particular length or scale* is relevant to the engineering performance over displacements of the same relative magnitude.

The relevance per se of the standard deviation of angle is less clear. However, it can probably be best appreciated if the distribution of angles is conceptualised as a probability density function. The gaussian assumption of angle distribution connotes a 16% probability that chord angles or asperities in excess of 1 standard deviation will exist in the profile. From Eq. (2), and assuming JCS $= 10\sigma_n$, the value of JRC is effectively the dilation angle at peak shear strength. It is noted that the dilation angle must be related to the inclination of the joint asperities in contact. Given the demonstrated correspondence between JRC and s_θ, it can be assumed that for JCS $= 10\sigma_n$, 16% of the profile is involved in the shearing process at peak shear strength. If a smaller percentage of the profile were involved (i.e. only steeper asperity angles), individual stresses on the asperities would be sufficient to either fail these asperities or to cause elastic deformations which would allow further asperities to come into contact; i.e. reinvolve lower angle asperities and reduce the dilation angle. The effect of varying the normal stress is discussed in the following section.

The Effects of Normal Stress

Barton and Choubey's empirical relationship (Eq. (2)) shows that the JRC value is multiplied by a logarithmic stress ratio factor to account for the effects of normal stress on dilation angle. This ratio will be equal to 1 and therefore have a neutral effect on JRC, when the joint wall compressive strength (JCS) is 10 times the applied normal stress (σ_n). The foregoing discussion of the percentage of asperities involved in the shearing process, is, therefore, dependent on the value of $\log(\text{JCS}/\sigma_n)$ being one.

The influence of the stress level on the effective dilation angle, as proposed by Barton and Choubey, is at least intuitively obvious. A higher normal stress on the

joint, would be expected to result in a lower dilation angle, as predicted by Eq. (2). The converse would be true for a lower normal stress.

It follows then, that at low normal stresses, less asperities will be in contact, and therefore involved in the shearing process, than at high normal stresses. Logan and Teufel (1986) established an approximately linear relationship between actual area of joint contact and normal stress for Tennessee sandstone and Indiana limestone. This linear relationship is adopted, and combined with the probabilistic concept introduced above. If the normal stress is reduced from 1/10 to 1/100 of the joint wall compressive strength, then the percentage of asperities involved at peak shear strength is predicted to reduce from 16% to 1.6%. Similarly, for a further ten-fold reduction in stress, only 0.16% of the asperities will be involved. As noted above, the 16% probability corresponds to 1 standard deviation. The 1.6% probability is equivalent to 2.1 standard deviations, and the 0.16% probability corresponds to 2.9 standard deviations. These effective dilation angle multipliers are very close to the predictions of 1.0, 2.0 and 3.0 given by Barton and Choubey's logarithmic stress-correction factor. An alternative basis for the empirically derived stress factor is therefore suggested.

Scale Effects of Joint Length

As noted earlier, the JRC value is scale dependent; larger joint samples were found to have lower apparent JRC values. Barton and Choubey (1977) suggested that as the joint length is increased, the inherent stiffness of the surrounding rock results in the joint wall contact being transferred to the major and less steeply inclined asperities as peak strength is approached. Bandis et al. (1983) recommended the use of natural block sizes for testing. Barton and Bandis (1982) recommended the following expression for scale correction of JRC, where subscripts $(_o)$ and $(_n)$ refer to laboratory scale (100 mm) and in-situ block sizes respectively:

$$\mathrm{JRC}_n \approx \mathrm{JRC}_o \left[\frac{L_n}{L_o}\right]^{-0.02\,\mathrm{JRC}_o}. \tag{24}$$

Barton and Bandis (1982) also recommend a similar scale correction for JCS.

The need for such a correction to JRC can best be appreciated by using the analogy of the mid-point displacement technique. The shear behaviour of longer joints may be controlled by longer asperities that are not evident in smaller sections of the joint. This is evident from the tests of Barton and Bandis (1982) where the displacement to peak was found to increase as the samples became longer. Bandis et al. (1981) note that the displacement to peak is approximately 1% of sample length. As the standard JRC value is assessed only relative to a standard 100 mm joint length, it is relevant only to the short asperities of approximately 1 mm length.

The following example is indicative, rather than rigorous, but serves to demonstrate the predicted influence of scale on JRC using fractal concepts. If the JRC value assessed on the basis of a 100 mm sample is 7, Eq. (24) suggests the empirically-corrected JRC for the 500 mm length should be 5.59. This correction can also be evaluated using fractal concepts. From above, the critical asperity

chord length is approximately 1% of sample length. For convenience, a chord length of 0.78 mm is adopted for the 100 mm long sample. This coincides with $N = 128$ (or 2^7) chords. Assuming equivalence of s_θ and JRC, the fractal dimension for this profile can be computed from Eq. (12) as $D = 1.001544$. As found by Bandis et al. (1981), the displacement to peak is proportional to sample length. In terms of the fractal model, this implies that the controlling asperities for longer profiles are proportionally longer. The JRC for the 500 mm joint can therefore be determined using a chord length of $500/128 = 3.90$ mm, from which $N = 100/3.9 = 25.6$. Reapplying this reduced value of N and the known value of D to Eq. (12) gives $s_\theta = 5.73°$, which is very close to the empirically-corrected JRC value of 5.59.

Similar comparisons for lower and higher JRC values are not quite so favourable, with a tendency for undercorrection for higher JRC values and overcorrection for lower values. It must be stressed, however, that this simplistic analysis, and indeed the JRC-JCS model, takes no account of the true complexities of joint roughness. Despite this, it can be appreciated that the fractal model provides an alternative basis for understanding the JRC-JCS scale corrections.

The Application of the Fractal Model to the Prediction of Shear Behaviour

The discussion of the JRC-JCS model has been presented as a validation of the applicability and potential of the fractal model, rather than as a justification of the empirical JRC-JCS model per se. It is the view of the authors, that the prediction of the shear behaviour of rough rock joints should rather be based on a fundamental theoretical understanding of the interface failure mechanisms.

The shear behaviour of rock joints is dependent not only on the geometry of the joint, which can be described by the fractal model, but also on the strength characteristics and elastic properties of the rock, and the prevailing boundary conditions. All of these considerations must be combined to describe the shear performance of a rock joint. Such an approach has been proposed by Seidel (1993), but a detailed description is beyond the scope of this paper.

7. Conclusions

In this paper it has been argued that it is unsatisfactory to characterise joint roughness as a single, discrete statistic; rather roughness must be represented as a continuous function of scale. It has been shown that such a representation can be achieved using the concepts of fractal geometry, in particular fractal dimensions and self-similarity. These concepts have been used as a basis for the formulation of a practical and statistically based model of roughness. This model has led to the derivation of important relationships between the fractal dimension and the standard deviation of both asperity angles and asperity heights, which in turn have been shown to provide a theoretical understanding of Barton's empirical JRC-JCS model. In particular, a relationship between JRC and s_θ has been suggested. In

addition, alternative bases for understanding the effects of normal stress on the shear performance of rough joints and the scale-dependence have been proposed.

Acknowledgments

The authors gratefully acknowledge funding of this work by the Australian Research Council, and the financial support for Dr. Seidel's PhD candidature by the Sir James McNeil Foundation.

References

Bandis, S., Lumsden, A. C., Barton, N. R. (1981): Experimental studies of scale effects on the shear behaviour of rock joints. Int. J. Rock Mech. Min. Sci. Geomech. Abstr. (18), 1–21.

Bandis, S., Lumsden, A. C., Barton, N. R. (1983): Fundamentals of rock joint deformation. Int. J. Rock Mech. Min. Sci. Geomech. Abstr. 20 (6), 249–268.

Barton, N., Bandis, S. (1982): Effects of block size on the shear behaviour of jointed rock. 23rd U.S. Symp. on Rock Mechanics, Berkeley, CA, 739–760.

Barton, N., Bandis, S. (1990): Review of predictive capabilities of JRC-JCS model in engineering practice. In: Proc., Int. Symp. on Rock Joints, Loen, Norway, Balkema, Rotterdam.

Barton, N., Choubey, V. (1977): The shear strength of rock joints in theory and practice. Rock Mech. 10, 1–54.

Brown, S. R. (1987): A note on the description of surface roughness using fractal dimension. Geophysical Research Letters 14 (11), 1095–1098.

Carr, J. R., Warriner, J. B. (1987): Rock mass classification using fractal dimension. In: Proc., 28th U.S. Symposium on Rock Mechanics, Tucson, Balkema, Rotterdam, 73–80.

Feker, E., Rengers, N. (1971): Measurement of large scale roughness of rock planes by means of profilograph and geological compass. Rock fracture, In: Proc., Int. Symp. on Rock Mechanics, Nancy.

Haberfield, C. M., Johnston, I. W. (1994): A mechanistically based model for rough rock joints. Accepted for publication Int. J. Rock Mech. Min. Sci. Geomech. Abstr.

Huang, S. L., Oelfke, S. M., Speck, R. C. (1992): Applicability of fractal characterization and modelling to rock joint profiles. Int. J. Rock Mech. Min. Sci. Geomech. Abstr. 29 (2), 89–98.

ISRM (1978): Suggested methods for the quantitative description of discontinuities in rock masses. Int. J. Rock Mech. Min. Sci. 15 (6), 319–368.

Kaye, B. H. (1989): A random walk through fractal dimensions, VCH Weinheim.

Kodikara, J. K. (1989): Shear behaviour of rock-concrete joints and side resistance of piles in weak rock. PhD Dissertation, Dept. of Civil Engng., Monash University.

Koura, M. M., Omar, M. A. (1981): The effect of surface parameters on friction. Wear 73, 235–246.

Krahn, J., Morgenstern, N. R. (1979): The ultimate frictional resistance of rock discontinuities. Int. J. Rock Mech. Min. Sci. 16, 127–133.

Lam, T. S. K. (1983): Shear behaviour of concrete-rock joints. PhD Dissertation, Dept. of Civil Engng., Monash University.

Lee, Y. H., Carr, J. R., Barr, D. J., Haas, C. J. (1990): The fractal dimension as a measure of the roughness of rock discontinuity profiles. Int. J. Rock Mech. Min. Sci. Geomech. Abstr. 27 (6), 453–464.

Leong, E. C., Randolph, M. F. (1992): A model for rock interfacial behaviour. Rock Mech. Rock Engng. 25 (3) 187–206.

Logan, J. M., Teufel, L. W. (1986): Effect of normal stress on the real area of contact. Pure Appl. Geophys. 124 (3), 471–485.

Mandelbrot, B. B. (1977): Fractals: form, chance and dimension, Freeman, San Francisco.

Mandelbrot, B. B. (1983): The fractal geometry of nature, Freeman, San Francisco.

Mandelbrot, B. B. (1985): Self-affine fractals and fractal dimensions. Physica Scripta 32, 257–260.

Patton, F. D. (1966): Multiple modes of shear failure in rock. In: Proc., 1st Congress Int. Soc. Rock Mechanics, Lisbon, 1, 509–513.

Reeves, M. J. (1985): Rock surface roughness and frictional strength. Int. J. Rock Mech. Min. Sci. Geomech. Abstr. 22 (6), 429–442.

Rengers, N. (1970): Influence of surface roughness on the friction properties of rock planes. In: Proc., 2nd Congress Int. Soc. Rock Mechanics, Belgrade, 1, 1–31.

Richardson, L. F. (1961): The problem of contiguity: an appendix of statistics of deadly quarrels. General Systems Yearbook 6, 139–187.

Seidel, J. P. (1993): The analysis and design of pile shafts in weak rock. PhD Dissertation, Dept. of Civil Engng., Monash University.

Stevens, R. F. (1990): Fractal programming in Turbo Pascal, M and T Publishing Inc., Redwood City, CA.

Tse, R., Cruden, D. M. (1979): Estimating joint roughness coefficients. Int. J. Rock Mech. Min. Sci. 16, 303–307.

Turk, N., Greig, M. J., Dearman, W. R., Amin, F. F. (1987): Characterization of rock joint surfaces by fractal dimension. In: Proc., 28th U.S. Symp. on Rock Mechanics, Tucson, Balkema, Rotterdam, 1223–1236.

Williams, A. F. (1980): The design and performance of piles socketed into weak rock. PhD Dissertation, Dept. Civil Engng., Monash University.

Wu, T. H., Ali, E. M. (1978): Statistical representation of joint roughness. Int. J. Rock Mech. Min. Sci. 15 (5), 259–262.

Yu, X., Vayassade, B. (1991): Joint profiles and their roughness parameters. Int. J. Rock Mech. Min. Sci. Geomech. Abstr. 28 (4), 333–336.

Authors' address: Dr. Chris Haberfield, Department of Civil Engineering, Monash University, Clayton, Victoria, 3168 Australia.